SURFACE DYNAMICS OF A RUBBER COVERED PULLEY

Brett DeVries

Flexible Steel Lacing Company (FLEXCO)

1. INTRODUCTION

The conveyor belt pulley plays a vital role in heavy industry. Continuous improvement in its design and manufacture has substantially increased reliability and capacity. However, the work of the pulley ultimately must be accomplished at the outer surface where it engages the conveyor belt. For many years rubber lagging has been bonded to the pulley surface to improve this engagement via enhanced friction coefficient, but the manner in which the friction arises is complex and poorly understood, as evidenced by slip failures to this day. Another role of pulley lagging is to act as a sacrificial layer protecting the expensive pulley. Naturally, there is strong interest in extending the life of the lagging, which requires knowledge of processes that cause abrasion to it. There are also several designs and thicknesses of lagging available and knowledge of the interaction dynamics would clarify the selection process.

Industry has long adopted standardised, uniform friction coefficients for rubber lagging. While they are a useful design tool, it is widely acknowledged that rubber does not behave with a simple, universal coefficient of friction. A recent study[8] showed that friction coefficient decreased with increasing pressure at a given slip distance. Other studies[6, 7] of rubber friction in tyres have described a complex frictional nature, where the rubber friction coefficient depends on slip history, contact pressure, and road asperity size due to viscoelastic energy dissipation in the rubber. This study sought to record generated friction coefficients as a function of pulley rotation to reveal the underlying timing and evolution of lagging friction while driving a conveyor belt.

Belt displacement, wrap pressure, and lagging shear angle were all measured as a function of pulley position as the pulley rotated through a 180° wrap angle. By measuring belt displacement, detailed data could be gathered near the belt entry and exit points where wrap pressure had not yet developed and lagging shear strain has been reported[5] to have large reversals. Belt displacements could also be correlated to belt shrinkage indicated by decreasing wrap pressure, and compared against lagging shear angle data to show slip areas. Wrap pressure was measured and used as a proxy for belt tension, but it also was needed to be able to calculate local coefficient of friction from the shear angle data. The technique for measuring shear angle differed from previous reports and contained variations.

Groundbreaking work by Zeddies[5] captured shear stress and wrap pressure under both laboratory conditions and in the field. The laboratory data supports a symmetrical pressure curve and shear stress plot, which were generated using steel cord belt and apparently solid rubber lagging. A detailed mechanism for generating this phenomenon was described[7]. However, the effect was not seen in this study, which used ply belts have modulus ratings in the order of 100 times less and also utilising an oversized pulley and highly grooved rubber lagging.

2. EXPERIMENTAL

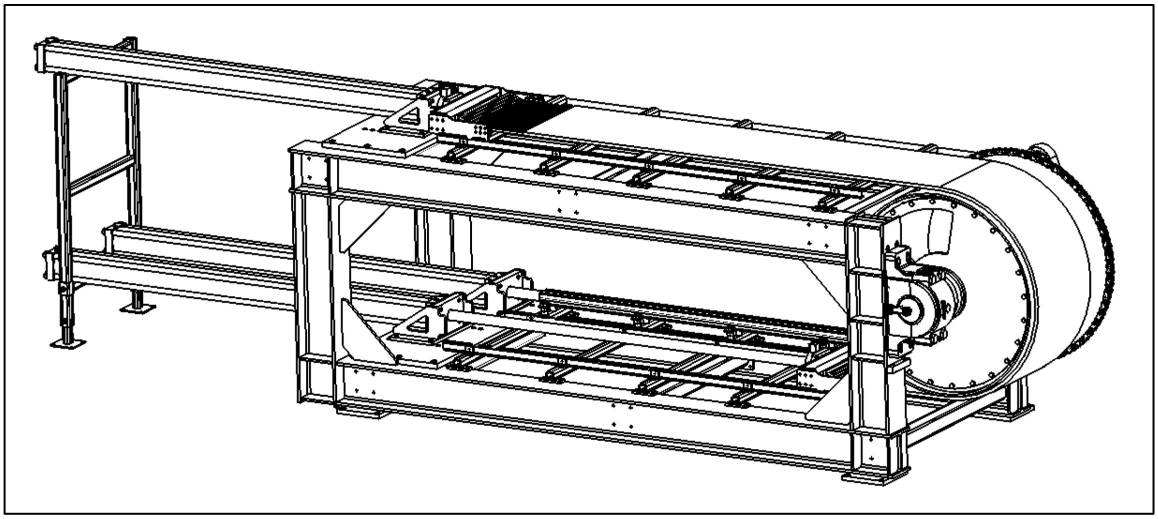

Figure. 1. Experimental setup illustrating the hydraulic tensioning system. The third cylinder rotated the pulley by retracting the wrapped leaf chain.

A hydraulically tensioned test rig was constructed (Figure 1). It was designed to measure wrap pressure, lagging shear angle movement and absolute belt displacement for various lagging and belt types on a pulley being rotated through a 180° wrap angle. Data collection began approximately 10° before the entry nip point (Top Dead Centre) and continued until 10° past the exit nip point. Each tension cylinder had a 50 kN load cell to measure force. To separately measure the lagging shear stain and the belt movement, mechanical sensor elements were installed inside a custom 1 219 mm diameter pulley. The pulley was installed in a steel framework such that hydraulic cylinders could apply adjustable T1 and T2 tensions while the pulley was rotated. Due to the slow speed of the test, the measurements were considered to be nearly static. An average test took approximately two minutes.

The hydraulic pressure in each cylinder was controlled with an adjustable spring based relief valve. These valves were limited in precision for setting initial test parameters and also suffered from pressure changes due to fluid flow in the control manifold once test motions began. To compensate, the cylinder load cells were necessary to accurately record force data throughout the test and were used to reliably verify the tension ratios described in each test result. However, some nominal variation in the starting tension was assumed for each set.

One wall of the pulley could be removed to facilitate installation on measurement devices inside the pulley. Two arrays were mounted inside, each consisting of a lagging shear angle sensor, a wrap pressure sensor, and a belt displacement sensor (Figures 2—4). Small holes were cut in the pulley shell for the sensors to acquire data.

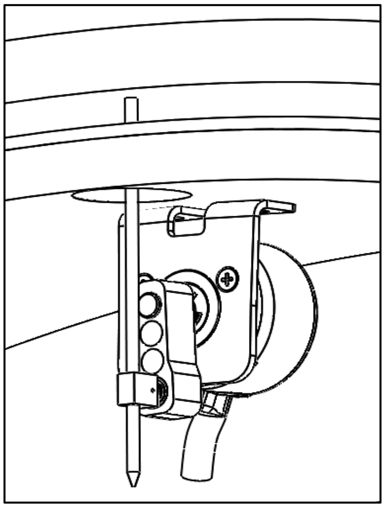

Figure. 2 Shear angle sensor sensor

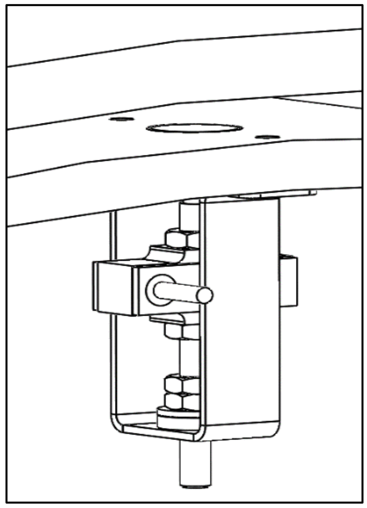

Figure 3. Wrap pressure sensor

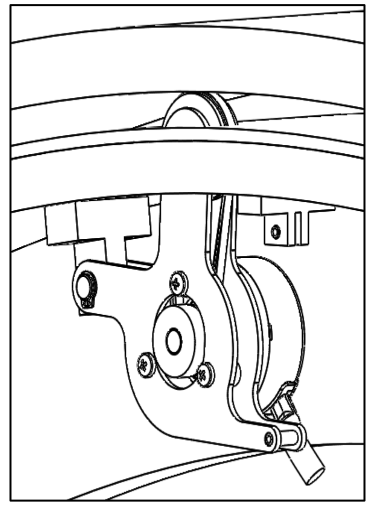

Figure 4. Belt displacement

The lagging shear indicator (Figure 2) consisted of a steel pin inserted into the rubber lagging (not shown) and received into a cone-shaped aperture in the pulley shell. Mounted to the pin was a UHMW slider that was attached to a rotatable low mass arm. This arm was secured to a 5 000 count rotary encoder. The angular movement of the pin could be derived from the arm movement using the below formula:

$$\theta = \sin^{-1}\left(\frac{r\sin\alpha}{\sqrt{r^2 + L^2 + 2rL\cos\alpha}}\right) \qquad 1$$

Where

r is the centre to centre length of the arm
L is the distance from the pulley surface to the center of encoder rotation
α is the rotation angle of the encoder

The wrap pressure sensor (Figure 3) consisted of a small load cell and a circular foot that pressed against the underside of the lagging layer. small preload was applied to assure positive contact and subtracted from the results.

Belt displacement measured the movement of the belt as compared to the pulley steel surface using the position of the belt when the pulley was at top dead centre, or 0° rotation, as the reference point. The belt displacement sensor) consisted of a 5 000 count encoder connected in a 2:1 ratio to an idler wheel via a miniature toothed belt to assure near zero slip between the wheels (Figure 4). The entire sensor pivoted on an axle to ensure positive contact with the belt and was held in contact via a tension spring (not shown). This mounting arrangement caused the idler wheel to protrude above the lagging layer prior to engagement with the belt. As the sensor array rotated to the entry nip point, the wheel would be depressed until flush with the lagging.

However, this would create rotation of the wheel prior to pulley and belt contact. Due to this, data prior to 0° and after 180° pulley rotation was removed from the resulting graphs for clarity. The lagging bonded to the pulley was 100% rubber strip lagging with extensive longitudinal channels and grooves (Figure 5). It was positioned on the pulley so that the shear measuring pin could be inserted approximately in the middle of one of the large diamonds.

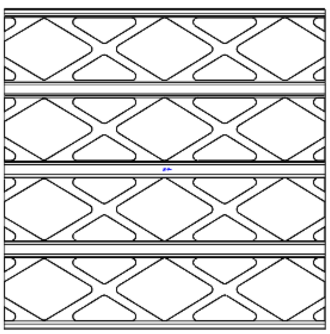
Figure 5. Diamond pattern rubber lagging.

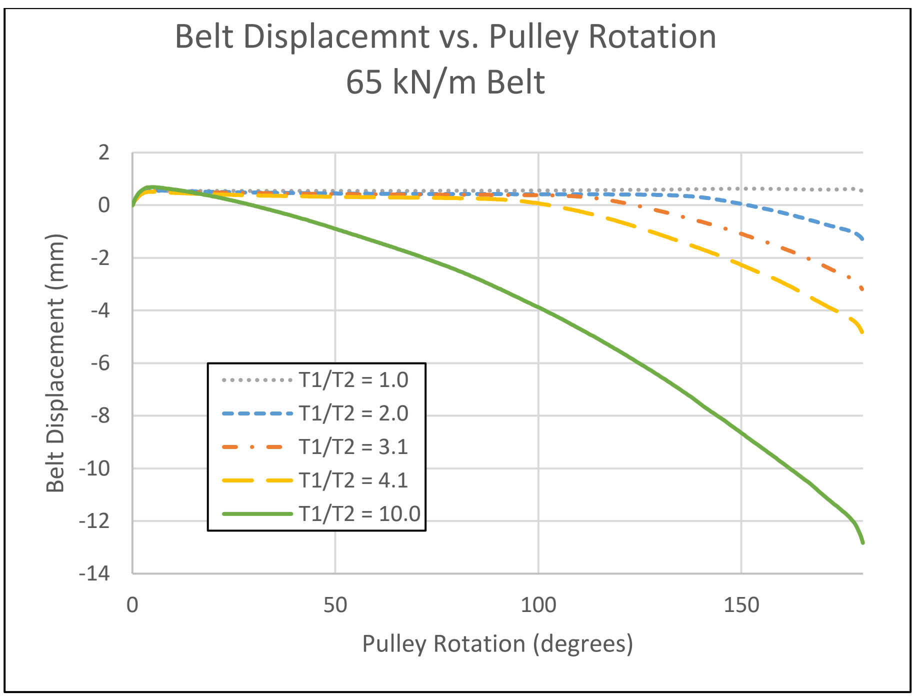

Figure 6. Belt displacement as a function pulley rotation angle for 609 mm wide, 11.1 mm thick belt with 1.6 mm cover thickness at various tension ratios.

3. RESULTS AND DISCUSSION

A 609 mm wide, 11.1 mm thick, two-ply, 65 kN/m rubber belt, with 4.8 mm top cover and 1.6 mm bottom cover was tested at various tension ratios. Plots were made depicting belt displacement or movement for various tension ratios (Figure 6). Negative values represent belt movement in the opposite direction to pulley rotation. Increased ratios caused an increase in the belt movement in a non-linear fashion. A major contribution to the increase was belt shrinkage and the growth of the active arc. The larger ratios require more of the wrapped angle to sustain the tension change, thereby applying the tension change to a longer section of belt, which results in greater shrinkage.

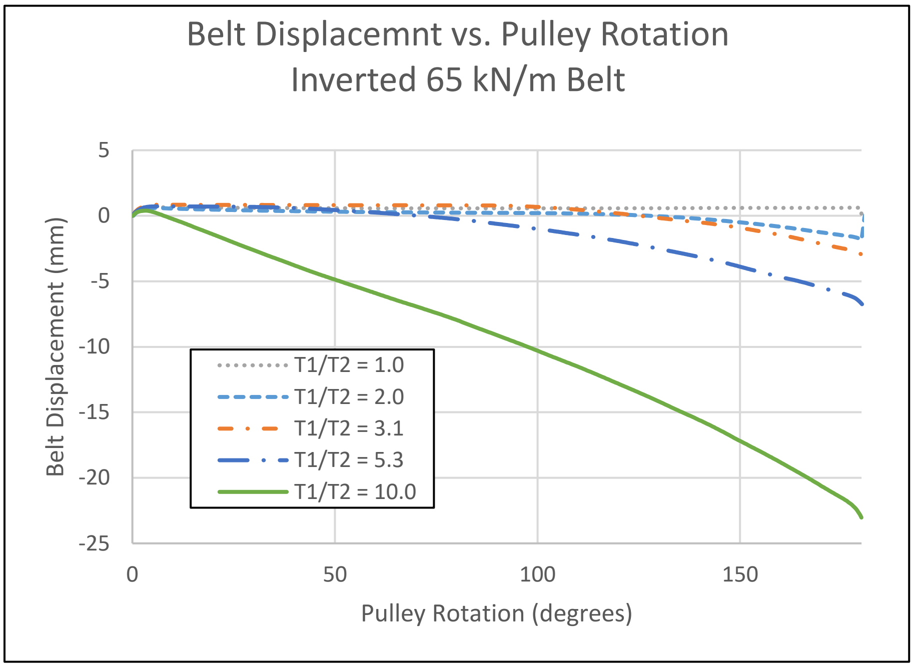

Figure 7. Belt displacement as a function pulley rotation angle for 609 mm wide, 11.1 mm thick belt with 4.8 mm cover thickness at various tension ratios.

This same belt was then inverted with the top cover facing the pulley to see the effects of increasing the bottom cover thickness. The Inverted Belt Displacement plot (Figure 7) again shows greater displacement as ratio increases. Comparison of the 3.1:1 ratios shows nearly identical displacements between the two tests. However, the inverted belt has twice the displacement at the 10:1 ratio. Reasons for this are unclear at this time.

Heavier construction belt was also tested. A 609 mm wide, 22.2 mm thick, four-ply, 175 kN/m rubber belt, with 6.4 mm top and bottom covers was tested at various tension ratios (Figure 8). This heavier belt experienced the onset of slip earlier than the 65 kN/m belt at the same ratio. It also was not able to reach the 10.0 ratio due to the onset of full macro slip. This demonstrates that the effective coefficient of friction is lower for the higher tension belt. This was due to lower friction coefficients predicted by the increased wrap pressure[7].

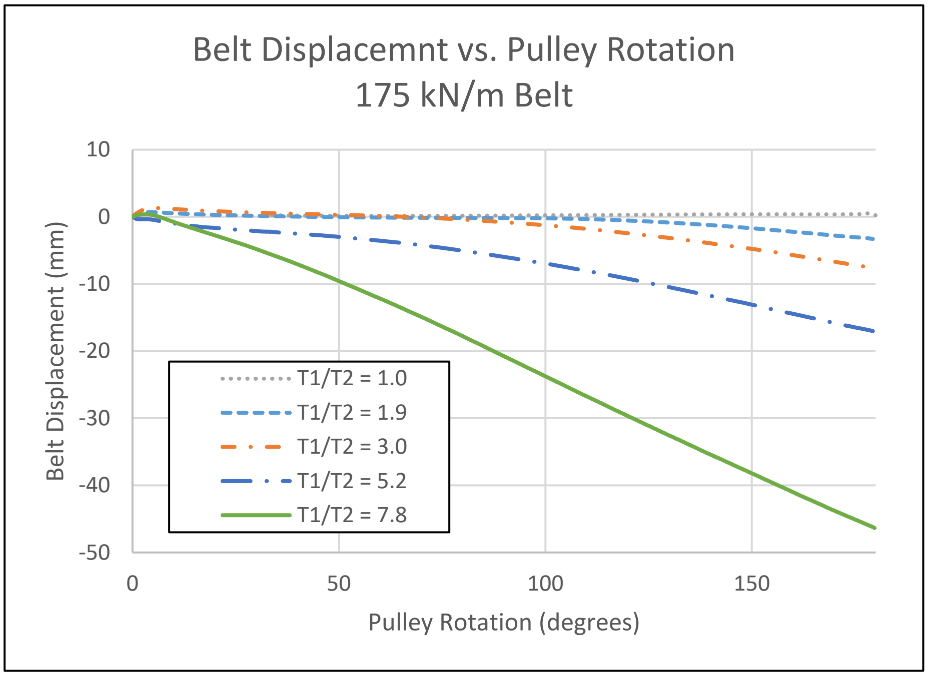

Figure 8. Belt displacement as a function pulley rotation angle for 609 mm wide, 22.2 mm thick belt with 6.4 mm cover thickness at various tension ratios.

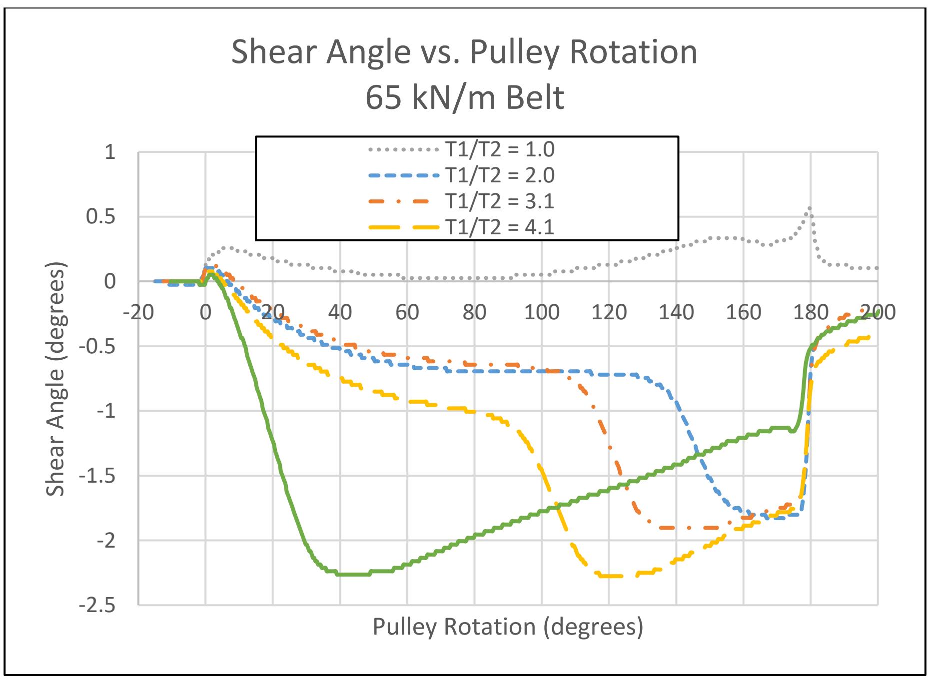

Figure 9. Measured shear angle in lagging layer as a function of pulley rotation angle 609 mm wide, 11.1 mm thick belt with 1.6 mm cover thickness at various tension ratios.

Lagging shear was also measured for the same three belt configurations. Lagging shear is of interest because it indicates the presence and magnitude of shear stress applied to the lagging surface. For these plots a positive shear angle corresponds to a shear stress in the direction of pulley rotation. The first feature observed on the shear plots (Figures 9–11) is the small positive rise on the 'driven' curves which peaks at approximately five degrees of pulley rotation. This small peak arises due to compression of the lagging itself. Since the belt is now moving about a smaller diameter, there is a slight reduction in the circumference. This results in the belt overrunning the original position until the lagging has finished compressing. It should be noted that this overrunning occurs prior to full wrap pressure, so it has little effect from a wear or friction standpoint.

A second feature common to mid-ratio shear plots is a quick reversal in the shear angle which then seems to stabilize (Figure 9). This feature is correlated in the displacement plots, but the movement is small, < .25 mm. Examination of the wrap pressure plots shows a slight cresting of the pressure and by necessity, tension. As the lagging is reacting to the torque being applied to the pulley, the negative shear angle in the lagging is accompanied by a backsliding movement and generates a corresponding slight increase in belt tension.

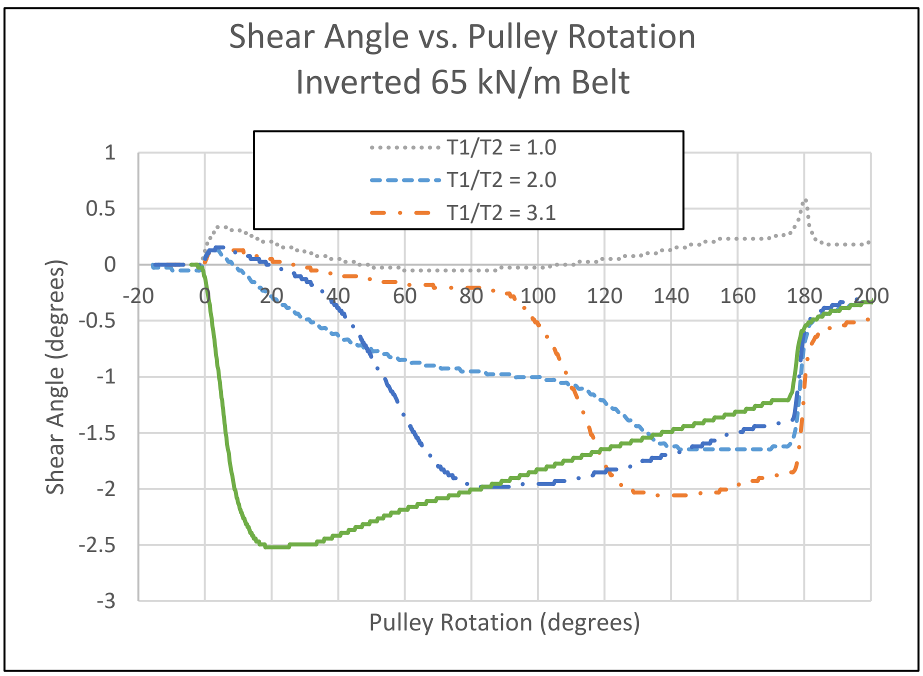

Figure 10. Measured shear angle in lagging layer as a function of pulley rotation angle 609 mm wide, 11.1 mm thick belt with 4.8 mm cover thickness at various tension ratios.

The third feature of the shear plot is the knee in the curve (Figures 9–10). This is the onset of the active arc. It is correlated by the start of negative displacement motion and by the onset of wrap pressure decrease. Negative displacement arises due to belt shrinkage due to tension removal from the belt. Initially this displacement increases the lagging shear angle until a maximum point is reached when the decreasing wrap pressure and the local coefficient of friction are in balance in the lagging shear stain and shear modulus. Belt movement at this stage is entirely in a slip regime. Greater tension ratios require larger active arcs and induce more slip.

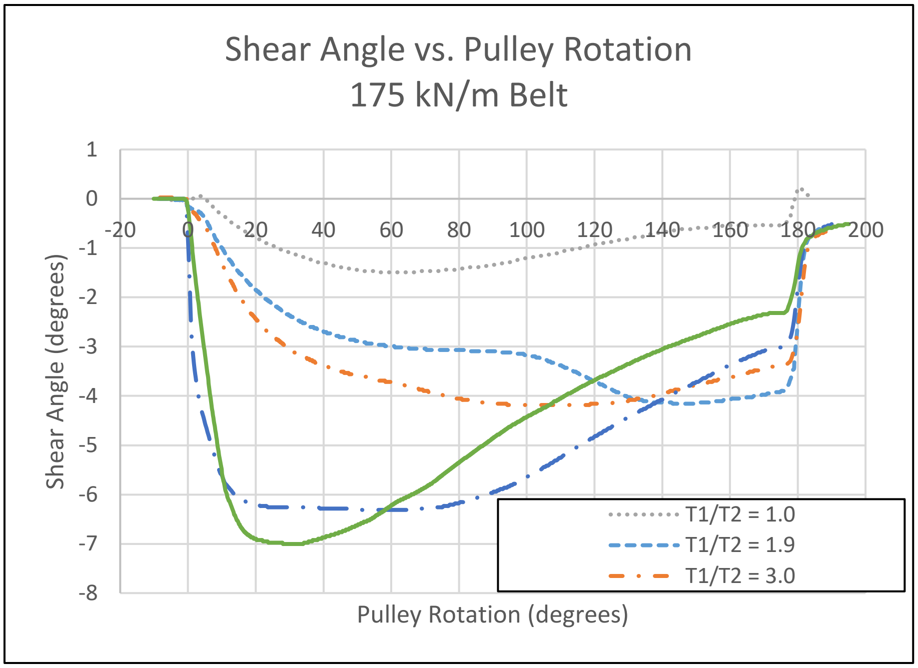

Figure 11. Measured shear angle in lagging layer as a function pulley rotation angle for 609 mm wide, 22.2 mm thick belt with 6.4 mm cover thickness at various tension ratios.

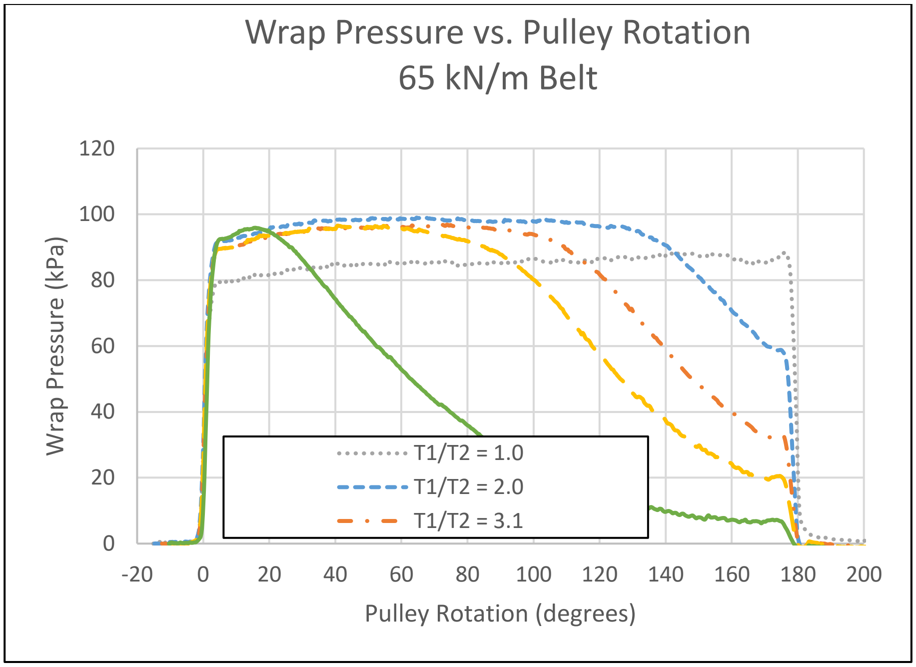

Figure 12. Wrap pressure as a function pulley rotation angle for 609 mm wide, 11.1 mm thick belt with 1.6 mm cover thickness at various tension ratios.

On the wrap pressure plots, full wrap pressure is not developed until roughly five degrees of rotation have occurred. There is a similar feature at the exit point of the pulley. There is also a corresponding decrease in the shear plots five degrees prior to the exit point of the belt. This feature has been previously identified and associated bending forces required to deflect the belt carcass[5], but belts tested were all steel cable construction and pulley diameters near the minimum recommended. Both would create relatively large bending forces. In this test, the pulley used exceeded the minimum pulley diameter by more than 250%, and the belt was a low modulus, fabric ply belt. This should minimise bending forces, and yet the effect remained. This indicates that the effect is independent of pulley diameter or belt construction.

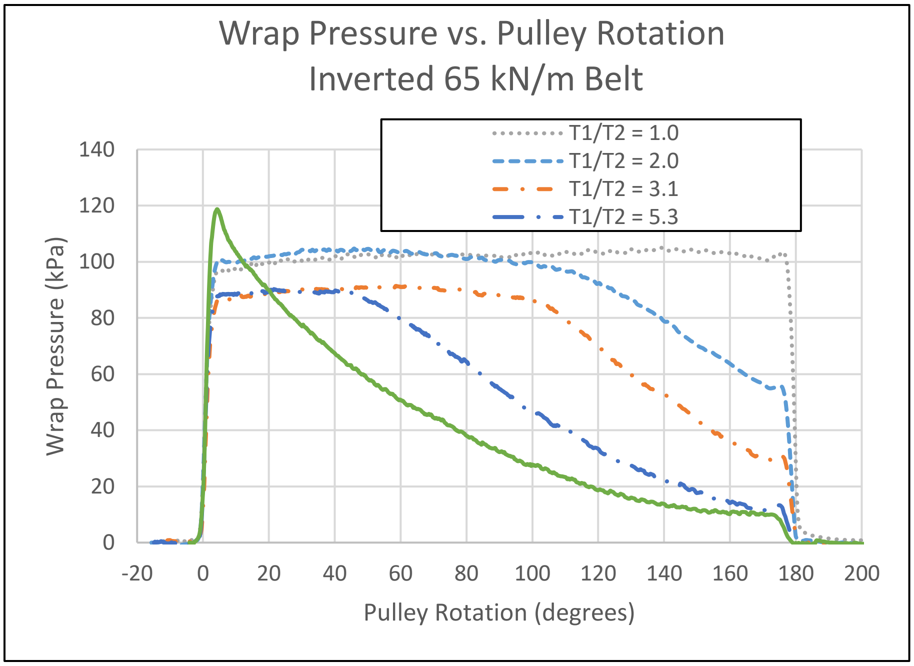

Figure 13. Wrap pressure as a function of pulley rotation angle 609mm wide, 11.1mm thick belt with 4.8mm cover thickness at various tension ratios.

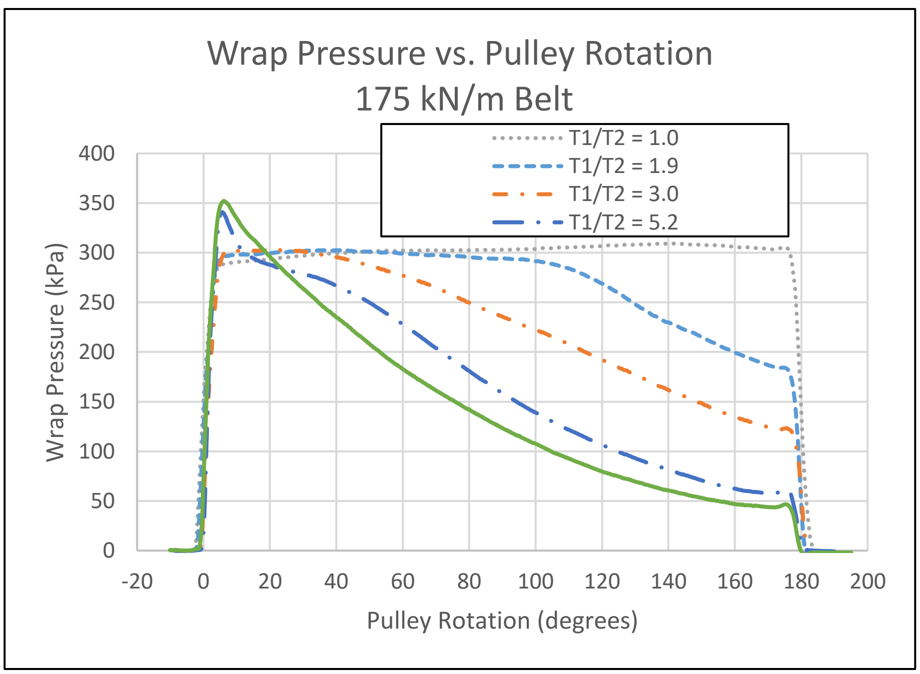

Figure 14. Wrap pressure as a function pulley rotation angle for 609 mm wide, 22.2 mm thick belt with 6.4 mm cover thickness at various tension ratios.

The data supported the following observations:

There is good support for the Wrap Pressure equation:

$$Wrap\ Pressure = \frac{2 * Tension}{Belt\ Width * Pulley\ Diameter} \qquad 2$$

Hence, pressure gradients are a good proxy for tension changes.

- Contrary to Zeddies[5], shear strain was not symmetrical about the midpoint of the wrap angle. This can be explained if the surface speed of the pulley is fractionally slower than the belt.
- For the 175 kN/m 1:1: ratio plot, there is a negative spike in the shear stress prior to the entry nip point and a positive spike after the exit nip point. This supports the prediction by Zeddies[5] that the rubber lagging layer is bulging beyond the nip points due to wrap pressure. It is not found in 65 kN/m belt, probably due to the lower wrap pressure.
- The sharp negative belt displacements that occur during the end of the pulley rotation can be compared against the displacement predicted by belt shrinkage. For example, the T1/T2 = 3.1 plot of the 65 kN/m belt has a displacement change of 2.33 mm from 105° to 175° rotation. The length of belt comprising an arc of 70° is 759.4 mm. The spring factor per unit width is (belt modulus/belt length), which is (6129.4 kN/m/m)/(.7594m) = 8070 kN/m. The tension change is found by T1 = 65.7 kN/m and T1/T2 = 3.1, (T1-T2) solves to give total tension change of 44.5 kN/m. However, the average tension change experienced by the belt is half that. Using the spring formula F=kx, (44.5 kN/m)(.5)(.6096m) = (8070 kN/m)*x. Calculated shrinkage is 1.68 mm for a difference of .65 mm.
- Even though there was no macro scale breakaway evident, clearly the large accumulated negative belt displacement in the maximum ratio plots indicate the lagging/belt interface had entered a regime of stick-slip frictional behavior. Stick slip is not a stable friction regime and material contamination, moisture, or rubber aging would all prevent these ratios from being used in practice.

4. COEFFICIENT OF FRICTION

Another goal of this project was to measure coefficient of friction as a function of pulley position. Recently, several research papers concerned with tyre friction behaviour have linked the origin of rubber friction to slip history, temperature, and contact pressure[3], [6]. Since both slip history and pressure have been measured in this study, an examination of the resultant friction is possible.

Since the displacements are small and the SBR based lagging rubber is fully cured and carbon-black filled, the lagging was approximated as an isotropic material that follows Hooke's law.

Therefore, shear stress should be proportional to shear strain:

$$\tau = G\gamma \qquad 3$$

Where

G is the shear modulus of the rubber

Rubber usually is considered to have a complex shear modulus, G(ω) +G'(ω). However, in this situation the speed is very slow and the strain values are small so G has been approximated as (.33)E, where elastic modulus (E) was measured at 10% elongation.

Furthermore, shear stress is a result of friction shearing the surface of the lagging.

$$\tau = \mu * (pressure) \qquad 4$$

Coefficient of friction was calculated as a function pulley rotation for all three belts (Figures 15–17) using the above equations.

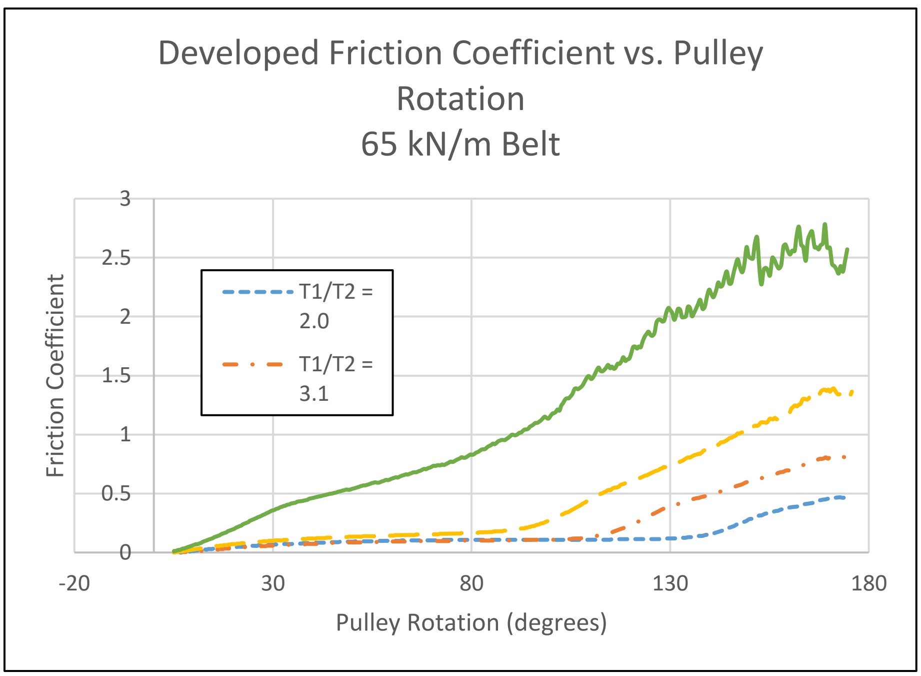

Figure 15. Developed friction coefficient as a function of pulley rotation angle for 609 mm wide, 11.1 mm thick belt with 1.6 mm cover thickness at various tension ratios.

The trend is for the friction to increase with the rotation angle. On the low ratio plots, the friction coefficient developed is initially small through the passive arc, and then rises quickly during the active arc. This is expected since the slip distance is increasing which is predicted to generate larger friction coefficients[3, 6]. However, the capacity for the rubber lagging to sustain traction while under diminishing pressures was substantial. Both of the 65 kN/m belts show very high friction coefficients for the T1/T2 = 10.0 plots. These values are best explained by an adhesion model of rubber friction, and would be compromised by the presence of dust, moisture or a lowering of the rubber surface energy by aging.

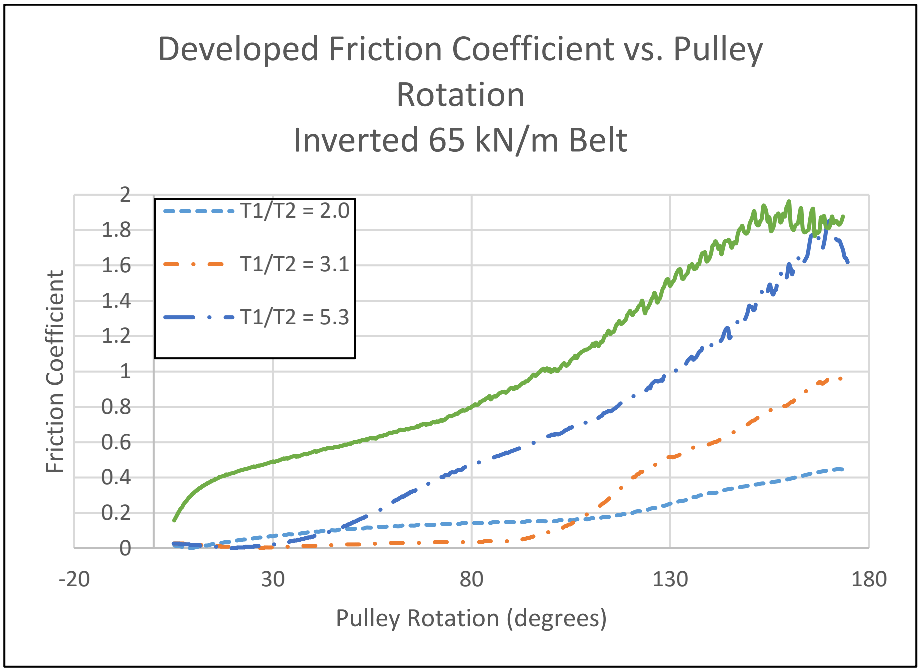

Figure 16. Developed friction coefficient as a function of pulley rotation angle for 609 mm wide, 11.1 mm thick belt with 4.8 mm cover thickness at various tension ratios.

The friction data shows a strong dependence on wrap pressure. Examination of the 2.0 ratio friction plots shows maximum friction for the 175 kN/m belt of .32, while the average max friction of the 65 kN/m belt was .45. This was despite the 175 kN/m belt displacing twice the amount of the 65 kN/m inverted belt and more than 3.5 times the

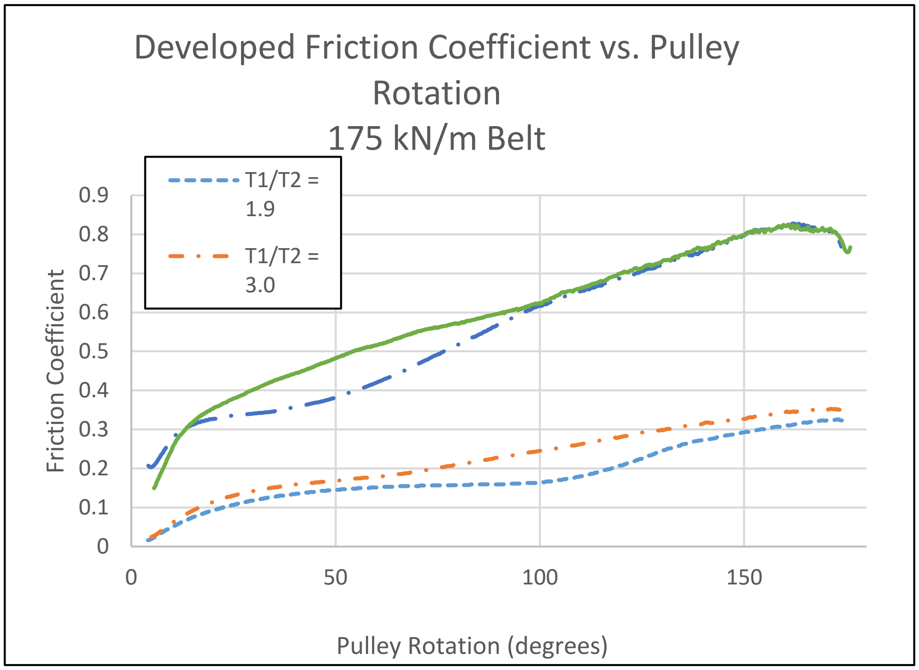

Figure 17. Developed friction coefficient as a function of pulley rotation angle for 609 mm wide, 22.2 mm thick belt with 6.4 mm cover thickness at various tension ratios.

regular 65 kN/m belt. However, the evidence for slip distance influence is also present. On the 65kN/m friction plot, the increase in friction between 140° and 180° is .3. The predicted friction increase due to pressure reduction based on DeVries[8] is only .1, so the remaining .2 increase is due to slip distance.

The method for predicting lagging friction now seems circular and iterative. First, tension is changed in the belt during the active arc[2]. The length of the active arc depends on the wrap pressure and friction developed, which generates surface traction to change the tension. Greater tension ratios require longer active arcs. But the active arc friction is dependent on wrap pressure and slip distance due to belt shrinkage. Belt shrinkage is calculated using the belt modulus, active arc length, and tension change, which is back to the start.

This complex process gives rise to the measured friction coefficients, which developed in response to the demands of the system. The result is the robust drive system that has been successfully deployed worldwide. As demands vary, the active arc length changes and more or less friction is developed while utilising more or less slip and thereby, wear.

ACKNOWLEDGEMENTS

The author gratefully acknowledges the expertise and assistance of Mr. Ross VanderWeide for the purchase and setup of the electronics and measurement software used to conduct the tests.

REFERENCES

1 Bowden, F., & Tabor, D. (1939). The area of contact between stationary and between moving surfaces. *Proc. R. Soc. A, 169*, 391-413.

Metlovic, P. M. (1996). *Mechanics of Rubber Covered Conveyor Rollers.* Akron, OH: Ph.D. Dissertation: The University of Akron.

Persson, B. (1998). On the theory of rubber friction. *Surface Science, 401*, 445-454.

4 Gabriel, P., Thomas, A., & Busfield, J. (2010). Influence of interface geometry on rubber friction. Wear, 268(5), 747-750.

5 Zeddies, H. (1987). Investigation of the Strain on Drum Laggings aiming the Optimization of the Lagging. Braunkohle, 39, 226

6 Heinrich G., Kluppel M. (2008). Rubber Friction, tread deformation and tire traction. Wear, 265, 1052-1060

7 Perrson, B. (2011). Rubber friction and tire dynamics. J. Phys,: Condens. Matter **23**, 015003

8 DeVries, B. (2015). Varient Lagging Friction Coefficents and Implications. IMHC Beltcon 18

ABOUT THE AUTHOR

BRETT DeVRIES

Mr. Brett DeVries is a staff engineer of research and development for conveyor belt accessories at Flexible Steel Lacing Company (FLEXCO), a US-based multinational company specialising in maximising belt conveyor productivity. Mr. DeVries holds a Bachelor of Science in mechanical engineering degree from Calvin College in Grand Rapids, Michigan and is a registered professional engineer by the State of Michigan. As an inventor, Mr. DeVries has 25 patents and is an active member in Conveyor Equipment Manufacturers Association (CEMA), Society for Mining, Metallurgy & Exploration (SME), and ASME.

BRETT DeVRIES

Flexible Steel Lacing (Flexco), USA